$^{19}F/^{29}Si$ Distance Determinations in Fluoride-Containing Octadecasil from Solid-State NMR Measurements

Colin A. Fyfe,* Andrew R. Lewis, Jean Michel Chézeau,[†] and Hiltrud Grondey

Contribution from the Department of Chemistry, University of British Columbia, 2036 Main Mall, Vancouver, British Columbia, Canada V6T 1Z1

Received January 21, 1997. Revised Manuscript Received July 9, 1997[⊗]

Abstract: In the present work we report results from CP, REDOR, and TEDOR NMR experiments carried out to locate the fluoride anions within the three-dimensional framework of the silicate octadecasil. Accurate Si−F distances were obtained through measurements of the $^{19}F/^{29}Si$ dipolar couplings from these experiments. Weighted, nonlinear least-squares fittings of the REDOR and TEDOR data for the silicons in the D4R units gave an average value of **D** = 1150 ± 50 Hz from which the Si−F interatomic distance was calculated to be 2.69 ± 0.04 Å. This distance is in excellent agreement with the value of 2.63 Å reported from the X-ray determined single crystal structure and confirms that the F^- anions are located inside the D4R units. Calculations and fittings of the REDOR and TEDOR data for the silicons not in the D4R gave **D** = 120 ± 20 Hz when the specific geometrical (tetrahedral) arrangement of the multiple equivalent fluoride anions surrounding the Si nuclei in these T-2 sites was taken into account. This yields a Si−F distance of 5.7 ± 0.4 Å, compared to the value 5.69 Å obtained from the diffraction measurements. Factors influencing the selection of the optimum experiments to perform in different situations and the dependence of the results on experimental variables are discussed. These studies clearly establish the viability and reliability of $^{19}F/^{29}Si$ REDOR and TEDOR NMR experiments to obtain distance information which can be used to determine the precise location of fluorine-containing species within such framework structures or in suitable cases to assist in the determination of the framework structure itself where it is unknown.

Introduction

Microporous materials such as zeolites are built up from corner-sharing [SiO₄] and [AlO₄]⁻ tetrahedra. Their framework structures contain regular systems of cavities and channels of molecular dimensions (3−13 Å) which are critical in the application of these materials as sorbents, catalysts, and molecular sieves.[1−4] One of their most important characteristics is the size and shape selectivity which they display toward sorbed organic molecules. This selectivity controls their catalytic reactions and product distributions as well as the selective adsorption of nonreactive molecules. Thus, there is considerable interest in investigating the detailed three-dimensional structures of zeolite frameworks containing intercalated species in order to understand in detail the nature of these sorbate-framework interactions.

There is, however, relatively little direct experimental information regarding the exact location of sorbed molecules within these frameworks. Although a considerable number of theoretical calculations have been carried out, the results are not always in agreement. For example, several groups have reported simulations for *p*-xylene absorbed in zeolite ZSM-5,[5−7] and these

reveal that the location found for the sorbate is very dependent on the type of calculation performed. Unfortunately it is very difficult to determine these structures experimentally by single crystal X-ray diffraction because it is necessary to have a single crystal which is large enough and which also contains a single sorbate in a well-defined stoichiometry, since in some cases the structures are known to be dependent on the loading of the guest molecule.[8,9] Although several structures have been solved for as-synthesized microporous materials where the location of the organic template has been determined, even these are sometimes ambiguous.[10−12] To date, only four detailed single crystal structures which locate sorbed organic guest molecules in the framework have been reported, all involving the ZSM-5 (MFI) framework.[13−16] Thus, other techniques must be developed to obtain this structural information.

In recent years we have worked to develop appropriate protocols for solid-state nuclear magnetic resonance (NMR) investigations of microcrystalline molecular sieve systems, with the ultimate aim of being able to determine both the 3-D structures of microporous frameworks and also their complexes with sorbed organic molecules. Here we present results from

* To whom correspondence should be addressed.

† Permanent address: Laboratoire de Matériaux Minéraux, URA 428 CNRS, Ecole Nationale Supérieure de Chimie de Mulhouse, 3 rue Alfred Werner F-68093, Mulhouse Cedex, France.

⊗ Abstract published in *Advance ACS Abstracts,* December 1, 1997.

(1) Breck, D. W. *Zeolite Molecular Sieves*; Wiley Interscience: 1974.

(2) Barrer, R. M. *Zeolite and Clay Materials as Sorbents and Molecular Sieves*; Academic Press: 1974.

(3) *Introduction to Zeolite Science and Practice*; van Bekkum, H., Flanigen, E. M., Jansen, J. C., Eds.; Elsevier: Amsterdam, 1991.

(4) *Advanced Zeolite Science and Applications*; Jansen, J. C., Stöcker, M., Karge, H. G., Weitkamp, J., Eds.; Elsevier: Amsterdam, 1994.

(5) Bell, R. G.; Lewis, D. W.; Voigt, P.; Freeman, C. M.; Thomas, J. M.; Catlow, C. R. A. *Stud. Surf. Sci. Catal.* **1994,** *84,* 2075.

(6) Cheetham, A. K.; Bull, L. M. *Catal. Lett.* **1992,** *13,* 267.

(7) Reischman, P. T.; Schmitt, K. D.; Olson, D. H. *J. Phys. Chem.* **1988,** *92,* 5165.

(8) Fyfe, C. A.; Strobl, H.; Kokotailo, G. T.; Kennedy, G. J.; Barlow, G. E. *J. Am. Chem. Soc.* **1988,** *110,* 3373.

(9) Fyfe, C. A.; Grondey, H.; Feng, Y.; Kokotailo. G. T. *J. Am. Chem. Soc.* **1990,** *112,* 8812.

(10) Price, G. D.; Pluth, J. J.; Smith, J. V.; Bennett, J. M.; Patton, R. L. *J. Am. Chem. Soc.* **1982,** *104,* 5971.

(11) van Koningsveld, H.; van Bekkum, H.; Jansen, J. C. *Acta Crystallogr.* **1987,** *B43,* 127.

(12) Mentzen, B. F.; Sacerdote-Peronnet, M.; Guth, J. L.; Kessler, H. C. R. *Acad. Sci. Paris* **1991,** *313,* 177.

(13) van Koningsveld, H.; Tuinstra, F.; van Bekkum, H.; Jansen, J. C. *Acta Crystallogr.* **1989,** *B45,* 423.

(14) van Koningsveld, H.; Jansen, J. C.; van Bekkum, H. *Acta Crystallogr.* **1996,** *B52,* 140.

(15) van Koningsveld, H.; Jansen, J. C.; de Man, A. J. M. *Acta Crystallogr.* **1996,** *B52,* 131.

(16) Reck, G.; Marlow, F.; Kornatowski, J.; Hill, W.; Caro, J. *J. Phys. Chem.* **1996,** *100,* 1698.

¹⁹F/²⁹Si Distance Determinations in Octadecasil

J. Am. Chem. Soc., Vol. 119, No. 50, 1997 12211

NMR experiments which locate the fluoride ions within the framework of octadecasil and demonstrate the feasibility of extending these experiments to other framework-host/fluorine-containing-guest systems.

The fluoride-synthesis route to molecular sieves originally developed by Flanigen and Patton[17] and extended by Guth and co-workers and others[18-21] produces very highly crystalline samples having high degrees of both long range and local ordering. This is indicated by the sharp reflections extending to high 2θ values which are observed in their X-ray powder diffraction patterns[22-24] and by the narrow resonances in their NMR spectra.[25] During the synthesis, fluoride anions can play several roles, acting as mineralizers, templates, or structure-directing agents.[18] Chemical analysis and ^{19}F MAS–NMR spectroscopy reveal that most of the as-synthesized materials have incorporated fluoride anions.[26]

However, it is often difficult to locate the fluoride ions by X-ray diffraction as the single crystals may be too small, or twinned, and recourse must be made to other techniques. There are additional complications in that fluorine and oxygen have very similar numbers of electrons making them difficult to distinguish, and F^- anions are isoelectronic with the OH groups which can occur as defects within these framework structures.[27] In several cases, however, fluoride anions have been clearly located in the double four-ring (D4R) units of the framework. These include octadecasil,[28] the tetragonal variant of AlPO$_4$-16,[29] three GaPO$_4$'s (cloverite,[30] GaPO$_4$-LTA,[31] and ULM-5[22]), and also an LTA-type AlPO$_4$ containing some cobalt and silicon.[32]

However the D4R moiety is not the only possible location; in the triclinic CHA-like ALPO$_4$-34,[23] and GaPO$_4$-34,[22] fluorine is part of the framework, and it apparently bridges two Al (or Ga) atoms. In AlPO$_4$-5, the fluoride anion has been located in the four-ring columns of the framework, far from the organic counterion.[33] In some cases it is not localized, and for purely

siliceous MFI-type zeolites a discrepancy exists: Price et al.[10] reported that the F^- was located close to the nitrogen of the tetrapropylammonium ion (TPA$^+$), while Mentzen[12] located it in the framework close to a four-ring but also found an unassigned site close to the TPA$^+$. In a few cases, such as the recently reported precursor of FER-type zeolite,[34] F^- is not incorporated, suggesting that its role in this case is restricted to that of a mobilizing agent. Thus, there is also interest in being able to locate the fluoride ions in these types of samples to improve understanding of the various roles they play in the syntheses.

Solid-state NMR in conjunction with Rietveld refinement of XRD data has been successfully demonstrated to be a powerful technique for the investigation of zeolite structures.[35,36] The ^{29}Si MAS–NMR spectra of highly siliceous zeolites can be directly related to the framework structure, the number and relative intensities of the resonances reflecting the numbers and occupancies of the crystallographically inequivalent T-sites in the asymmetric unit.[8,37,38] We have recently demonstrated the successful application of 2-D INADEQUATE NMR experiments to the assignment of the individual ^{29}Si resonances to specific T-sites in these frameworks as well as the determination of their complete three-dimensional connectivities.[9,36,37] This makes it possible, in principle, to determine the locations of species within the frameworks by determining the distances between their component atoms and specific T-sites in the framework.

Solid-state NMR spectroscopy has considerable potential in solid-state structure investigations via the direct determination of internuclear distances from experiments based on the through-space dipolar interactions between pairs of nuclei I and S. The dipolar coupling, D, between two nuclei depends on the gyromagnetic ratios of the two nuclei, γ_I, and γ_S, and on the I-S internuclear distance r through eq 1.

$$D = \mu_0 \gamma_I \gamma_S h / (8\pi^2 r^3) \qquad (1)$$

Here μ_0 is the permeability of free space and h is Planck's constant. Because of the strong power dependence of D on r, moderately accurate values of dipolar couplings can yield very accurate values for the corresponding internuclear distances, the most unambiguous distance measurements coming from experimental systems where I and S interact as isolated spin-pairs. The dipolar interaction is greatest for nuclei with high gyromagnetic ratios, making ^{19}F attractive for these studies. Furthermore, while the ^{19}F isotope is 100% abundant, fluorine is relatively uncommon in chemical systems, and thus the likelihood of potential background interferences is minimal.

In high-resolution solid-state NMR the sample is usually spun rapidly (2–20 kHz) about an axis inclined at 54.74° to the axis of the magnetic field. This is referred to as magic angle spinning (MAS) and has the desirable effect of narrowing the otherwise extremely broad (up to several kHz) resonances because, in addition to averaging the chemical shift to its isotropic value, the heteronuclear dipolar interactions for an isolated spin-pair

(17) Flanigen, E. M.; Patton, R. L. U.S. Patent No. 4073865, 1978.
(18) Kessler, H.; Patarin, J.; Schott-Darie, C. *Stud. Surf. Sci. Catal.* **1994**, *85*, 75.
(19) Guth, J. L.; Kessler, H.; Caullet, P.; Hazm, J.; Merrouche, A.; Patarin, J. In *Proceedings of the 9th International Zeolite Conference, Montreal, 1992*; von Ballmoos, R., Higgins, J. B., Treacy, M. M. J., Eds.; Butterworth-Heinemann: 1993; p 215.
(20) Zhao, D.; Qiu, S.; Pang, W. In *Proceedings of the 9th International Zeolite Conference, Montreal, 1992*; von Ballmoos, R., Higgins, J. B., Treacy, M. M. J., Eds.; Butterworth-Heinemann: 1993; Vol. 1, p 337.
(21) Loiseau, T.; Riou, D.; Taulelle, F.; Férey, G. *Stud. Surf. Sci. Catal.* **1994**, *84*, 395.
(22) Schott-Darie, C.; Kessler, H.; Soulard, M.; Gramlich, V.; Benazzi, E. *Stud. Surf. Sci. Catal.* **1994**, *84*, 101.
(23) Simmen, A. Ph.D. Thesis, E. T. H. Zurich, Switzerland, 1992.
(24) Simmen, J.; Patarin, J.; Baerlocher, Ch. In *Proceedings of the 9th International Zeolite Conference, Montreal, 1992*; von Ballmoos, R., Higgins, J. B., Treacy, M. M. J., Eds.; Butterworth-Heinemann: 1993; p 433.
(25) Chézeau, J. M.; Delmotte, L.; Guth, J. L.; Soulard, M. *Zeolites* **1989**, *9*, 78.
(26) Delmotte, L.; Soulard, M.; Guth, F.; Seive, A.; Lopez, A.; Guth, J. L.; *Zeolites* **1990**, *10*, 778.
(27) Védrine, J. C. In *Guidelines for Mastering the Properties of Molecular Sieves*; Barthomeuf, D., Derouane, E. G., Hölderich, W., Eds.; Plenum Press: New York, 1989; p 121.
(28) Caullet, P.; Guth, J. L.; Hazm, J.; Lamblin, J. M.; Gies, H. *Eur. J. Solid State Inorg. Chem.* **1991**, *28*, 345.
(29) Schott-Darie, C.; Patarin, J.; Le Goff, P. Y.; Kessler, H.; Benazzi, E. *Microporous Mater.* **1994**, *3*, 123.
(30) Estermann, M.; McCusker, L. B.; Baerlocher, C.; Merrouche, A.; Kessler, H. *Nature* **1991**, *352*, 320.
(31) Merrouche, A.; Patarin, J.; Soulard, M.; Kessler, H.; Anglerot, D. In *Synthesis of Microporous Materials*; Occelli, M. L., Robson, H. E., Eds.; Van Nostrand Reinhold: 1992; Vol. 1, p 384.
(32) Sierra, L.; Deroche, C.; Gies, H.; Guth, J. L. *Microporous Mater.* **1994**, *3*, 29.
(33) Qiu, S.; Pang, W.; Kessler, H.; Guth, J. L. *Zeolites* **1989**, *9*, 440.

(34) Schreyeck, L.; Caullet, P.; Mougenel, J.-C.; Guth, J. L.; Marler, B. *J. Chem. Soc., Chem. Commun.* **1995**, 2187.
(35) Fyfe, C. A.; Gies, H.; Feng, Y.; Kokotailo, G. T. *Nature* **1989**, *341*, 223.
(36) Fyfe, C. A.; Feng, Y.; Grondey, H.; Kokotailo, G. T.; Gies, H. *Chem. Rev.* **1991**, *91*, 1525.
(37) Fyfe, C. A.; Feng, Y.; Gies, H.; Grondey, H.; Kokotailo, G. T. *J. Am. Chem. Soc.* **1990**, *112*, 3264.
(38) Engelhardt, G.; Michel, D. *High-Resolution Solid-State NMR of Silicates and Zeolites*; John Wiley and Sons: New York, 1987.

are averaged to zero during each complete rotor cycle.[39,40] Thus, in its simplest form, the use of MAS precludes a direct measurement of *D*, although this interaction is responsible for the coherence transfer in the cross polarization (CP) process.[41,42] In those cases where the spin system behaves essentially as an isolated heteronuclear spin-pair, an oscillatory behavior in the amplitude of the CP signal at short contact times is observed for both nonrotating solid samples[42,43] and those undergoing magic angle spinning.[44] Such dipolar oscillations arise because the magnetization shuttles between the *I* and *S* spins and have been reported for several different systems under MAS conditions.[45–50] If the observed spins experience dipolar coupling to several heteronuclear spins, oscillations at several frequencies interfere and a smooth exponential rises to a maximum followed by a decay due to relaxation is typically observed.[41,46]

Recently, Schaefer and co-workers have introduced the Rotational-Echo DOuble Resonance (REDOR)[40,51] and Trans-ferred-Echo DOuble Resonance (TEDOR)[52,53] experiments which use radio frequency pulses applied at specific points in each rotor period to prevent the complete averaging out of the dipolar interactions and thus permit dipolar dephasing to occur. From these, the magnitude of the dipolar couplings can be experimentally determined using appropriate analyses,[53–57] and the interatomic distances can be accurately determined from the dipolar couplings (eq 1) for systems of isolated spin-pairs. The requirement of isolated spin-pairs has usually been met by isotopically labeling the molecules of interest (e.g., $^{13}C-^{15}N$ in natural compounds) and diluting these in a large excess of the unlabeled compound.[54,57,58]

REDOR and TEDOR distance determinations are more complicated if several nuclei contribute to the dephasing.[56,57,59] For example, the presence of natural abundance "background" spins can substantially influence the observed dephasing, especially when the nuclei under investigation have large gyromagnetic ratios.[57,59] Corrections for this may be made by subtracting the dephasing measured for a natural abundance sample[54] or by generating a model structure assuming an appropriate statistical and geometric distribution of dephasing spins and then calculating the multispin dephasing explicitly.[56,59] TEDOR and REDOR have been applied to amino acids,[51–54] peptides,[53,57,58] proteins,[60,61] semiconductors,[62] polymers,[63] and molecular sieve frameworks.[64–67] In cases where the distances are known independently from X-ray diffraction measurements, those obtained from REDOR and TEDOR experiments are in very good agreement.[54,58]

In the present work we present the results of Si–F distance measurements on as-synthesized octadecasil. Octadecasil, chosen to be representative of molecular sieve framework structures, is the purely siliceous analogue of $AlPO_4$-16 and was recently synthesized by Caullet et al.[28] from fluoride-containing media. The crystal structure was solved using single crystal X-ray methods, the fluoride anions located, and accurate Si–F distances determined.[28] The low natural abundance of ^{29}Si (4.7%) in the framework, combined with the weak homonuclear couplings means that the $^{19}F-^{29}Si$ dipolar interactions should approximate clusters of isolated heteronuclear spin-pairs for which theoretical TEDOR and REDOR behavior can be calculated. We demonstrate that octadecasil, which contains two distinct T-sites and two quite different Si–F interatomic distances, is an excellent model case for determining the best experiments to use as well as the optimization of these experiments and the subsequent analysis of the experimental data.

Experimental Section

Materials. The pure, highly crystalline octadecasil sample (crystal size 80 μm), kindly provided by Dr. P. Caullet, was prepared by hydrothermal synthesis from a fluoride-containing medium with qui-nuclidine (1-azabicyclo[2.2.2]octane, $[N(CH_2CH_2)_3CH]$) as template in the presence of HF.[28] After synthesis, the product was washed with distilled water and dried at 90 °C. The structure was checked by powder X-ray diffraction and ^{19}F and ^{29}Si MAS–NMR measurements, all of which agreed with previously reported results.[18,28,68] Carbon, nitrogen, and silicon contents were determined by elemental analysis. Calculated (weight %) for 100% occupancy: C, 11.48%, N, 1.9%, Si 38.4%, Found: C, 10.5%, N, 1.78%, Si, 38.12%. Fluorine contents in these materials are usually in the range 2.3–2.6%,[28] which corresponds to occupancies of 80–100% of the D4R units by fluoride ions. The idealized elemental composition of octadecasil is $Si_{20}O_{40}\cdot2(Q^+F^-)$ where Q^+ is the quinuclidinium cation.

NMR Experiments. The NMR experiments were performed on a Bruker MSL-400 spectrometer, operating at frequencies of 376.434 and 79.495 MHz for ^{19}F and ^{29}Si, respectively. The silicon frequency was generated by mixing a 400.13 MHz signal with a frequency-doubled 160.3175 MHz signal. Chemical shifts were referenced to external $CFCl_3$ for ^{19}F and to tetramethylsilane (TMS) for ^{29}Si using external Q_8M_8 (the cubic octamer $Si_8O_{12}[OSi(CH_3)_3]_8$) as an intermediate reference. A Bruker double-tuned $^1H/X$ MAS probe with the ^1H channel tuned to the ^{19}F frequency was used, and the sample was spun using either a Bruker 7-mm stator or a Doty Scientific 7-mm high-speed stator. Spinning speeds of 2.0–5.2 kHz were attainable. The

(39) Waugh, J. S.; Maricq, M. M.; Cantor, R. *J. Magn. Reson.* **1978**, *29*, 183.

(40) Gullion, T.; Schaefer, J. *Adv. Magn. Reson.* **1989**, *13*, 57.

(41) Voelkel, R. *Angew. Chem., Int. Ed. Engl.* **1988**, *27*, 1468.

(42) Stejskal, E. O.; Schaefer, J.; Waugh, J. S. *J. Magn. Reson.* **1977**, *28*, 105.

(43) Mehring, M. *Principles of High Resolution NMR in Solids*, 2nd ed.; Springer-Verlag: New York, 1983; Chapter 4.

(44) Hediger, S.; Meier, B. H.; Ernst, R. R. *J. Chem. Phys.* **1995**, *102*, 4000.

(45) Hagaman, E. W.; Ho, P. C.; Brown, L. L.; Schell, F. M.; Woody, M. C. *J. Am. Chem. Soc.* **1990**, *112*, 7445.

(46) Schaefer, J.; Stejskal, E. O.; Garbow, J. R.; McKay, R. A. *J. Magn. Reson.* **1984**, *59*, 150.

(47) Hawkes, G. E.; Mantle, M. D.; Sales, K. D.; Aime, S.; Gobetto, R.; Groombridge, C. J. *J. Magn. Reson. Ser. A* **1995**, *116*, 251.

(48) Hediger, S.; Meier, B. H.; Ernst, R. R *Chem. Phys. Lett.* **1995**, *240*, 449.

(49) Walther, K. L.; Wokaun, A.; Baiker, A. *Mol. Phys.* **1990**, *71*, 769.

(50) Klein Douwel, C. H.; Maas, W. E. J. R.; Veeman, W. S.; Werumeus Buning, G. H.; Vanken, J. M. J. *Macromol.* **1990**, *23*, 406.

(51) Gullion, T.; Schaefer, J. *J. Magn. Reson.* **1989**, *81*, 196.

(52) Hing, A. W.; Vega, S.; Schaefer, J. *J. Magn. Reson.* **1992**, *96*, 205.

(53) Hing, A. W.; Vega, S.; Schaefer, J. *J. Magn. Reson. Ser. A* **1993**, *103*, 151.

(54) Pan, Y.; Gullion, T.; Schaefer, J. *J. Magn. Reson.* **1990**, *90*, 330.

(55) Mueller, K. T. *J. Magn. Reson. Ser. A* **1995**, *113*, 81.

(56) Goetz, J. M.; Schaefer, J. *J. Magn. Reson.* **1997**, *127*, 147.

(57) Naito, A.; Nishimura, K.; Tuzi, S.; Saitô, H. *Chem. Phys. Lett.* **1994**, *229*, 506.

(58) Holl, S. M.; Marshall, G. R.; Beusen, D. D.; Kociolek, K.; Redlinski, A. S.; Leplawy, M. T.; McKay, R. A.; Vega, S.; Schaefer, J. *J. Am. Chem. Soc.* **1992**, *114*, 4830.

(59) McDowell, L. M.; Klug, C. A.; Beusen, D. D.; Schaefer, J. *Biochemistry* **1996**, *35*, 5395.

(60) Marshall, G. R.; Beusen, D. D.; Kociolek, K.; Redlinski, A. S.; Leplawy, M. T.; Pan, Y.; Schaefer, J. *J. Am. Chem. Soc.* **1990**, *112*, 963.

(61) McDowell, L. M.; Barkan, D.; Wilson, G. E.; Schaefer, J. *Solid State Nucl. Magn. Reson.* **1996**, *7*, 203.

(62) Holl, S.; Kowalewski, T.; Schaefer, J. *Solid State Nucl. Magn. Reson.* **1996**, *6*, 39.

(63) Pan, Y. *Solid State Nucl. Magn. Reson.* **1995**, *5*, 263.

(64) Fyfe, C. A.; Mueller, K. T.; Grondey, H.; Wong-Moon, K. C. *Chem. Phys. Lett.* **1992**, *199*, 198.

(65) Fyfe, C. A.; Mueller, K. T.; Grondey, H.; Wong-Moon, K. C. *J. Phys. Chem.* **1993**, *97*, 13484.

(66) Blumenfeld, A. L.; Coster, D.; Fripiat, J. J. *J. Phys. Chem.* **1995**, *99*, 15181.

(67) Fyfe, C. A.; Wong-Moon, K. C.; Huang, Y.; Grondey, H.; Mueller, K. T. *J. Phys. Chem.* **1995**, *99*, 8707.

(68) Marcuccilli Hoffner, F.; Delmotte, L.; Kessler, H. *Zeolites* **1993**, *13*, 60.

[19]F/[29]Si Distance Determinations in Octadecasil

J. Am. Chem. Soc., Vol. 119, No. 50, 1997 12213

Table 1. [19]F−[29]Si Spin-Pair Dipolar Couplings (*D*) Calculated for Various Si−F Interatomic Distances (*r*)[a]

r/Å	2.7754	2.7327	2.6925	2.6546	2.6329	**2.6300**	2.6258	2.5847
D/Hz	1050	1100	1150	1200	1230	**1234**	1240	1300
r/Å	6.0776	5.8875	5.8009	5.7192	**5.6878**	5.6419	5.5686	5.4328
D/Hz	100	110	115	120	**122**	125	130	140

[a] Boldface entries are for the distances and corresponding dipolar couplings calculated from the single crystal X-ray structure of octadecasil by Caullet et al.[28]

peak separations of the spinning sidebands in the ^{19}F MAS−NMR spectra were used to determine the spinning frequency, ν_r, to an accuracy of better than 10 Hz. The spinning speed was checked before and after each experiment and showed no measurable change. Knowledge of ν_r is required to calculate the rotor period (τ_r) and subsequently the various delays needed for precise positioning of the pulses in the TEDOR and REDOR experiments. Typically, $\pi/2$ pulses were in the range 6−10 μs corresponding to rf field strengths of 25.0−41.6 kHz.

Cross Polarization Experiments. For the cross polarization experiments the Hartmann-Hahn sideband matching condition[44,69] was established experimentally by fixing the ^{19}F radio-frequency power and adjusting the [29]Si radio-frequency power to maximize the observed signal. For variable contact time CP experiments, spectra were acquired using contact times from 10 μs to 60 ms. Dipolar interactions are modulated by the one and two times the spinning frequency under MAS conditions, and this leads to strong first and second order sidebands in the CP matching profile if the spinning speed exceeds the width of the abundant *I*-spin resonance line and the heteronuclear dipolar coupling frequency.[44] Because these CP matching sidebands become narrow at high spinning speeds, the sideband Hartmann-Hahn matching requires highly stable rf amplitudes and constant spinning rates over extended periods of time.

REDOR Experiments. In all the REDOR experiments the observed nucleus was [29]Si, and the trains of rotor-synchronous dephasing pulses were applied to [29]Si or ^{19}F, depending on the pulse sequence used (see below). The dephasing pulses were always timed to occur at half and full rotor periods, the ^{19}F offset was exactly on resonance, and the [29]Si frequency was set to be approximately midway between the two silicon resonances. In the REDOR experiments which incorporated an initial cross polarization from ^{19}F to [29]Si to improve the efficiency, a 10 ms contact time was used. To eliminate artifacts from the effect of small but finite switching times within the spectrometer, dephasing pulses were applied in both the S_0 and S_f experiments rather than removing the pulses for the S_0 as is normally done.[51,54] The desired effect of either reintroducing the dipolar interactions or not was then achieved by switching the frequency on and off resonance using a frequency offset list. A variety of null experiments confirmed that the 10 MHz offset employed was sufficiently large. For example, the difference signal was zero if both experiments were off resonance, as expected.

TEDOR Experiments. For TEDOR experiments the fluorine signal was set exactly on resonance, and the observed nucleus was [29]Si. The [29]Si frequency was set so that one of the silicon signals was on resonance. Null experiments performed without the transfer pulse showed that the observed signals arose from coherence transfer. Several different versions of the TEDOR experiment were used as will be discussed in detail later. These included applying the dephasing pulses on [29]Si or ^{19}F before the coherence transfer pulse, varying the spinning speed, the positions of the dephasing pulses, and incrementing the number of rotor cycles before or after the transfer pulse.

Data Analysis. Fitting to determine the relaxation times was carried out using the commercial Bruker software. Values of the expected [19]F−[29]Si dipolar coupling constants for a range of Si−F distances were calculated using eq 1 and are summarized in Table 1. The boldface entries in the table correspond to the experimental Si−F interatomic distances determined from the crystal structure data for octadecasil reported by Caullet et al.[28] and the corresponding dipolar couplings.

For the REDOR and TEDOR experiments, the heteronuclear [19]F−[29]Si dipolar couplings for the T-1 silicons were determined from weighted nonlinear least-squares fitting of the data in *Mathematica*[70] using the analytical functions reported by Mueller.[55] For all the REDOR

and TEDOR calculations the spins were assumed to be at fixed positions within a rigid lattice. Calculations for three-spin systems indicate virtually no difference between the dephasing calculated either including or neglecting the effects of homonuclear couplings, provided these interactions are significantly smaller than the magic angle spinning speed.[56,61] In the present work homonuclear dipolar interactions were ignored because the [19]F−[19]F couplings and the much weaker [29]Si−[29]Si couplings were much less than the sample spinning speeds employed (2−5 kHz).

For the analysis of TEDOR experiments the exact value of the dipolar coupling during the period before coherence transfer needs to be known in order to calculate the curve for the period after the transfer and vice versa. In real situations the coupling is not known *a priori* but can often be estimated by using known values for similar systems and, in the present case, even estimated from the (known) interatomic distances. It is advantageous to use the analytical functions[55] as these avoid more complex numerical calculations.

Prior to commencing nonlinear fitting, trial fittings were used to determine approximate values for the parameters that were not fixed in the experiment, the dipolar coupling and a scaling factor to match the experimental and theoretical intensities. For TEDOR experiments there is no normalization as there is for REDOR, so the scaling factor was arbitrary, and an exponential dampening factor was incorporated to take into account T_2 decay during the evolution period.[53] Weighted nonlinear fittings of the data were carried out starting from these initial parameter values, and these were constrained to realistic (positive) limits. The Levenberg−Marquardt algorithm[70] was utilized to minimize the value of the parameter $\chi^2 = \sum |F_i - f_i|^2$ where F_i is the value of the *i*th data point and f_i is the value obtained from the fit. The best values for the parameters were taken as those which gave the smallest χ^2 values. Because the spectra acquired for small numbers of rotor cycles had better signal-to-noise ratios, they yielded more accurate intensities, and consequently these data were given more emphasis during the fitting procedure. Several data-weighting schemes were evaluated, and weighting by the inverse of the number of rotor periods proved to be the most reliable, giving very reproducible results if the initial parameter values were varied.

For experiments where the positions of the pulses were not those used for the derivations of the analytical functions reported by Mueller,[55] and also when multiple spin analysis was required, the appropriate integrals[40,53,56] for the TEDOR and REDOR functions were determined and then evaluated using point-by-point numerical integration over a sphere to produce a powder average as described below.

Results and Discussion

Octadecasil Crystal Structure. The structure of octadecasil, the purely siliceous analogue of AlPO$_4$-16 (IZA Structure Commission Framework Code AST), has been solved by single crystal X-ray methods.[28] The framework consists of octadecahedral [4[6]6[12]] cages and hexahedral [4[6]] cages and can be built by linking the octadecahedra through all their common six-membered ring faces (Figure 1a). Since these octadecahedral cages do not completely fill three-dimensional space another type of void, the very small [4[6]]-cage or double four-membered ring (D4R) unit is created.

When prepared from a fluoride-containing medium, the as-synthesized product contains the quaternary ammonium templating cation (quinuclidinium in this case) in the large cages, and the negatively charged fluoride anion (needed to balance the positive charge of the organic cation) in the D4R units, and crystallizes in a tetragonal phase (symmetry group *I* 4/*m*, no.

(69) Hartmann, S. R.; Hahn, E. L. *Phys. Rev.* **1962**, *128*, 2042.

(70) Wolfram, S. *Mathematica. A System for Doing Mathematics by Computer*; Addison-Wesley: Massachusetts, 1991.
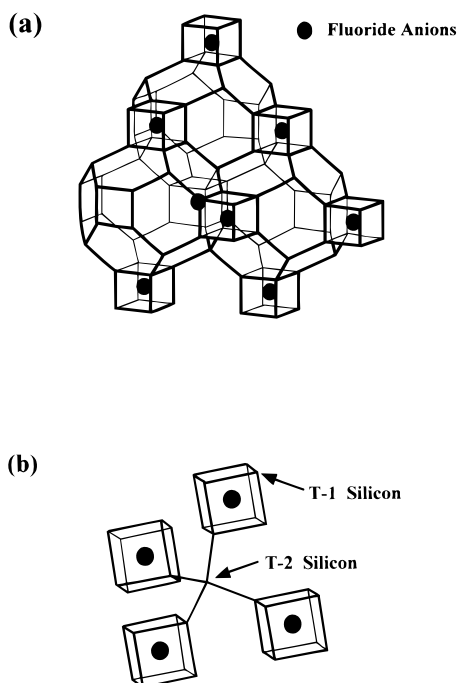
(a)

(b)

Figure 1. (a) Schematic representation of the framework structure of octadecasil showing the packing arrangement of the two types of cages, the large $[4^6 6^{12}]$-cages and the small $[4^6]$-cages (or D4R units). Silicon atoms lie at each vertex, and oxygen atoms are located approximately midway along the lines. Thick lines indicate connections closer to the viewer. The $[4^6 6^{12}]$-cages pack in a tetrahedral arrangement by sharing all their six-membered ring faces and $[4^6]$-cages fill the voids thus created. Fluoride anions lie at the center of ca. 90% of the double four-ring units. (b) Portion of the octadecasil framework showing the four D4R units surrounding each T-2 silicon. Each T-1 silicon is connected to three other T-1 sites in the same D4R unit and to one T-2 silicon. Fluoride anions are 2.63 Å from each T-1 silicon in the $[4^6]$-cage and 5.69 Å from the nearest T-2 silicon. The distance between fluoride anions in adjacent D4R units is 9.33 Å.

87).[28] The octadecasil structure contains two types of T-sites (Figure 1), T-1 sites at the vertices of the D4R units and T-2 sites located at the vertices of six-rings in the ratio 4 T-1:1 T-2. There are 20 [SiO$_4$] tetrahedra, and thus 16 T-1 and 4 T-2 sites per unit cell. Each T-2 links 4 T-1's from four different D4R units (Figure 1b). From the X-ray crystal structure data, the T-1 silicons are 2.63 Å from the fluoride ion inside their D4R unit and more than 7 Å from the fluoride ions in the adjacent D4R units. The T-2 silicons are 5.69 Å from each of four equivalent fluoride anions, and the closest F−F distance is 9.33 Å.

1-D ^{19}F and ^{29}Si NMR Experiments. Qualitative ^{19}F and ^{29}Si MAS−NMR spectra were in general agreement, both with previously reported data and the crystal structure as discussed above. In order to best implement the different experiments, a knowledge of the different nuclear relaxation parameters is essential. T_1 and T_2 were measured for both nuclei and are summarized in Table 2.

The room-temperature 1-D ^{19}F MAS−NMR spectrum (Figure 2a) shows a single resonance at −38.2 ppm with respect to CFCl$_3$. The chemical shift is indicative of a single, unique environment and is similar to those reported for other ^{19}F/^{29}Si systems where the fluoride ion is located within a D4R unit.[26,28] The static ^{19}F NMR spectrum consists of a single peak with a full-width at half-height (FWHH) of 6200 Hz. The room temperature 1-D ^{29}Si MAS−NMR spectrum of octadecasil shows two resonances at −107.7 and −111.6 ppm with respect to tetramethylsilane (TMS) (Figure 2b). These peaks have an

Table 2. ^{29}Si and ^{19}F MAS−NMR Relaxation-Time Measurements[c]

relaxation parameter	F$^-$ δ(CFCl$_3$) = −37.8 ppm	T-1 Si δ(TMS) = −108 ppm	T-2 Si δ(TMS) = −111 ppm
T_1[a]	2.6 s	22 s	20 s
T_2[a,b]	3.5 ms	18 ms	20 ms

[a] Values determined by fitting using the commercial Bruker software. [b] Data acquired with rotor-synchronization. [c] Performed at frequencies of 79.495 and 376.434 MHz, respectively.
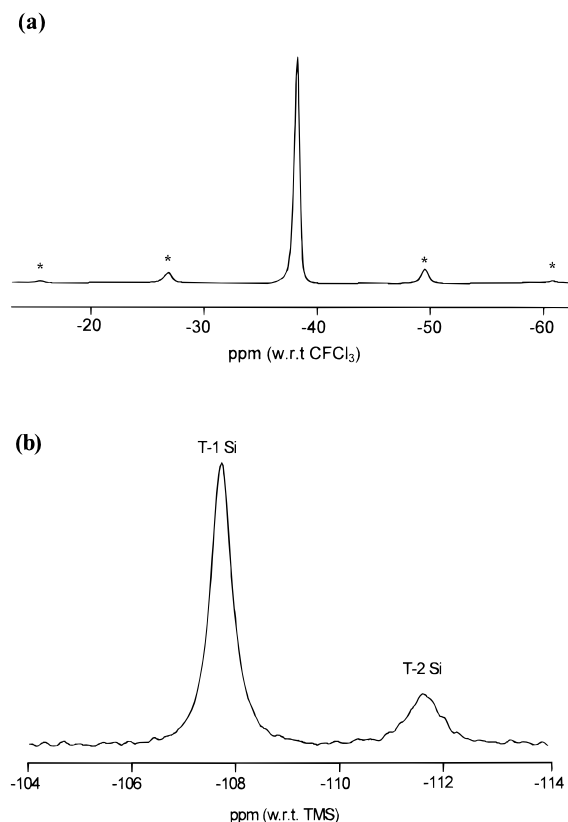
(a)

ppm (w.r.t CFCl$_3$)

(b)

ppm (w.r.t. TMS)

Figure 2. (a) ^{19}F MAS−NMR spectrum of octadecasil, obtained with 132 scans, spinning speed 4.296 kHz, pulse width 9 μs, relaxation delay 10 s (spinning sidebands marked *). (b) Quantitative ^{29}Si MAS−NMR spectrum of octadecasil showing the two resonances assigned to the T-1 and T-2 silicons, respectively. The relative peak intensities (4:1) are as expected from the crystal structure. The spectrum was acquired with 48 scans, spinning speed 2.2 kHz, pulse width 8 μs, relaxation delay 110 s, and no decoupling.

intensity ratio of 4:1 and are assigned to the silicons in the T-1 and T-2 sites, respectively.[28] The static ^{29}Si NMR spectrum shows a single resonance with a FWHH of 1700 Hz.

Clearly, the known framework structure of octadecasil containing fluoride anions in the D4R units with its two different Si−F interatomic distances and two distinct silicon environments provides an ideal test case for evaluating the reliability and robustness of ^{19}F/^{29}Si REDOR and TEDOR NMR experiments involving molecular sieve frameworks as well as for determining the optimum experimental conditions for them. For clarity the different experiments will be discussed separately.

^{19}F−^{29}Si Cross Polarization Experiments. In variable contact-time CP experiments, the ^{29}Si signal intensity is monitored as a function of the spin-locking time τ. The initial exponential build-up of intensity is usually characterized by the CP rate constant, T_{CP}^{-1}, as polarization is transferred from ^{19}F to ^{29}Si during the Hartmann-Hahn match.[43] An exponential decay with first order rate constant $T_{1\rho}^{-1}$ due to loss of the spin-locked magnetization via spin−lattice relaxation in the rotating

frame is superimposed on this growth. For a system of isolated spin-pairs, the magnetization transfer process via matched Hartmann-Hahn spin-locked cross polarization under MAS conditions should exhibit oscillatory behavior as the polarization shuttles between the connected spin-pairs,[44] as reported previously for a few cases.[45−50] Variable contact-time cross-polarization experiments from ^{19}F to ^{29}Si on octadecasil were carried out at several spinning speeds, and different behaviors were observed for the two types of T-sites.

For the T-1 silicons the variable contact time CP experiments showed a rise to a maximum, with a clear oscillatory behavior in the signal amplitude at short contact times, followed by an exponential decay (data not shown). On some occasions these oscillations were absent, and this was attributed to mismatching arising from variations in the rf power or the spinning speed during the course of the experiment. Because the silicons in the T-1 sites are very close (<3 Å) to the fluoride ion which occupies their D4R, and the next-nearest ^{19}F nuclei in adjacent D4R units are much further away (>7 Å), these silicons and their corresponding F$^{−}$ may be considered as isolated ^{19}F−^{29}Si spin-pairs. An oscillatory behavior is thus expected for the T-1 silicons; however, under MAS conditions the maintenance of the sideband Hartmann-Hahn match for CP necessitates extremely stable rf powers and spinning speed. For the T-2 silicons a smooth rise to a maximum followed by a decay was observed. Since the T-2 silicons are surrounded by up to four equidistant (5.69 Å) fluoride anions, they are not expected to show the oscillatory behavior predicted for isolated spin-pairs.

REDOR Experiments. In the REDOR pulse sequence, trains of rotor-synchronized π-pulses which reverse the sign of the dipolar coupling are applied to reintroduce the effects of the heteronuclear dipolar coupling that are normally removed by sample rotation at the magic angle. Two dephasing pulses per rotor cycle are needed to prevent the spinning from averaging the dipolar interactions to zero and to ensure the dephasing is accumulated.[40] Two experiments are performed, one with dephasing and one without. The echo intensity of the experiment where no dephasing occurs is denoted by S_0, while that of the smaller echo acquired under the influence of the reintroduced heteronuclear dipolar dephasing is labeled S_f. The intensity difference, $\Delta S = S_0 - S_f$, is due to the effect of the heteronuclear dipolar coupling. The normalized intensity ratio $\Delta S/S_0$ shows a nonperiodic oscillation when plotted against the number of rotor cycles, n, the evolution time, or the dimensionless parameter $\lambda = n\boldsymbol{D}\tau_r$,[40] where τ_r is the time for a complete rotor revolution. The phase accumulation from dipolar dephasing for an isolated heteronuclear spin-pair may be calculated by integrating over the time of the evolution to yield the normalized REDOR difference signal as defined by eq 2 with the integration limits $\alpha \in [0, 2\pi]$ and $\beta \in [0, \pi]$.[54]

$$\Delta S/S_0 = 1 - (4\pi)^{-1} \int \int \cos[\Delta\Phi(\alpha, \beta, \lambda)] \sin\beta \, d\beta \, d\alpha \quad (2)$$

Here α is the azimuthal angle and β is the polar angle defined by the internuclear vector in a coordinate system defined with the z axis parallel to the rotor axis as illustrated in Figure 3a. The factor of $(4\pi)^{-1}$ is required to normalize this integral, and the $\sin\beta$ is a geometrical weighting factor required to account for the statistical (spherical) distribution of the pairs of nuclei in a powder about the spinning axis. For two dephasing π-pulses per rotor cycle positioned at one-half and complete rotations of the spinner, the REDOR phase accumulation $\Delta\Phi$ is given by eq 3.[55]

$$\Delta\Phi(\alpha, \beta, \lambda) = (32)^{1/2} \lambda \sin\beta \cos\beta \sin\alpha \quad (3)$$
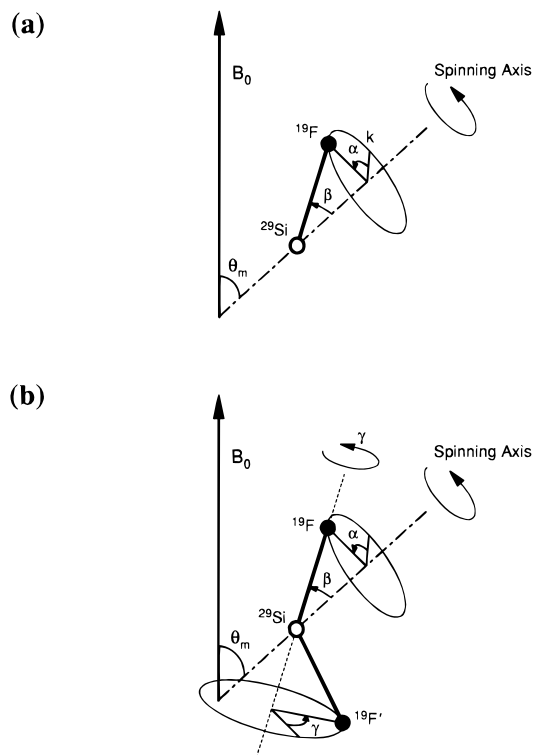

Figure 3. Definitions of the angles used to calculate the dipolar dephasing. (a) An isolated ^{29}Si−^{19}F internuclear vector under rotation about an axis inclined at the magic angle ($\theta_m = 54.74°$) to the static magnetic field B$_0$. The azimuthal angle $\alpha \in [0, 2\pi]$ is measured from the reference vector k in the plane normal to the rotation axis, and the polar angle $\beta \in [0, \pi]$ is the angle between the internuclear vector and the rotation axis. (b) For two or more ^{19}F nuclei interacting with a single ^{29}Si nucleus, three angles α, β, and γ are needed to describe all possible orientations of these in a powder sample that is spinning at the magic angle. The angles α and β are defined as for the isolated spin-pair, and $\gamma \in [0, 2\pi]$ defines rotation about a common chosen internuclear vector to produce all possible relative orientations of the internuclear vectors. The angles between the heteronuclear vectors are fixed because the nuclei are in a rigid lattice. This treatment can be readily extended to three or more ^{19}F nuclei. For actual calculations it is more convenient to parameterize this system in terms of the Euler angles ϕ, θ, and ψ (see text).

In a REDOR experiment the signal intensity is monitored as a function of either the number of rotor periods or the position during the rotor cycle at which the dephasing pulses are applied, with the number of rotor periods constant.[40] Commonly, a series of π dephasing pulses is applied to the unobserved heteronuclear spins, with a simple spin-echo sequence on the observed spins.[40] However when the resonance offsets are large, pulse errors can accumulate, and while phase-cycled pulse trains help to compensate for pulse imperfections, they too become ineffective at large offsets.[71] In such cases it is desirable to minimize the number of pulses on those nuclei having large offset effects. Garbow and Gullion[72] have reported a modified REDOR pulse sequence that requires only a single dipolar dephasing pulse on the unobserved heteronuclear spins to minimize these problems.

Several pulse sequence schemes were used to implement the REDOR experiments, two of which are presented in Figure 4: a sequence with a train of dephasing pulses on the unobserved (*I*) nuclei and a sequence with a single dephasing pulse on the unobserved nuclei. Because the REDOR experiment involves the formation of an echo for the observed nucleus, it is the spin−lattice relaxation behavior of this nucleus which determines how quickly the sequence can be repeated. As ^{29}Si was the observed

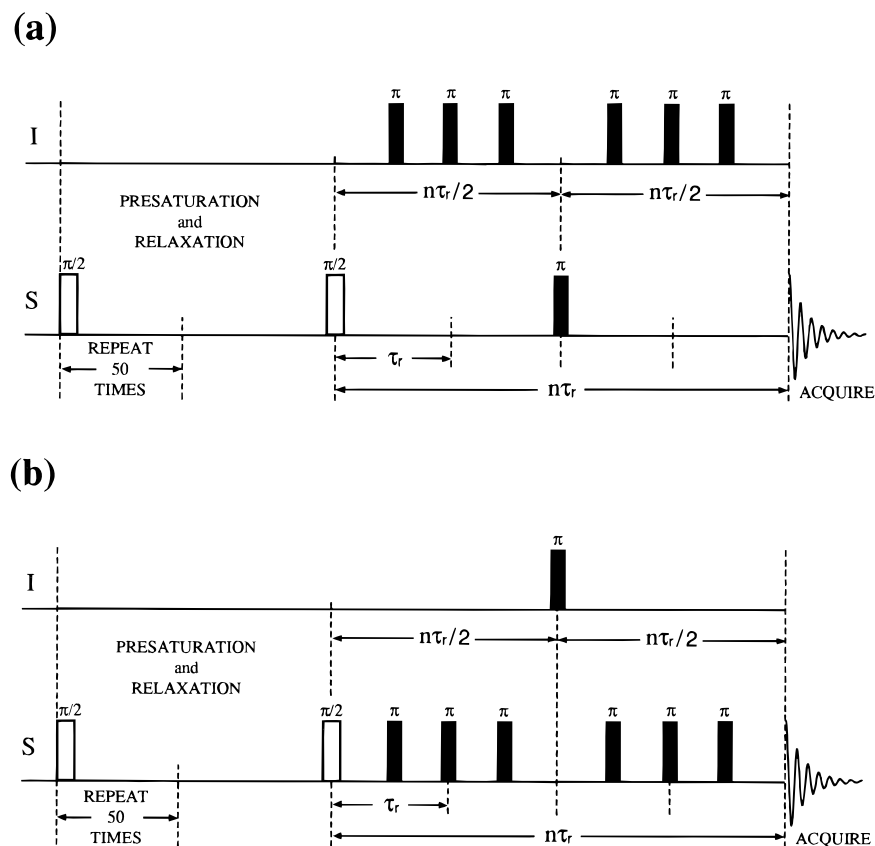(71) Gullion, T.; Schaefer, J. *J. Magn. Reson.* **1991**, *92*, 439.

(a)

(b)

Figure 4. REDOR pulse sequences with (a) dephasing π-pulses on unobserved nuclei and (b) a single π-pulse on the unobserved nuclei to minimize resonance offset effects. The dephasing pulses were positioned at half and full rotor periods, and n is the number of rotor cycles. The sequences shown are for $n = 4$, but n can be incremented from the minimum value of 2 by an even number of rotor periods. Because the T_1 relaxation times for the silicons in octadecasil are relatively long (ca. 20 s), an initial presaturation sequence was incorporated to allow a more efficient recycling time, while still ensuring quantitative reliability. In experiments which utilized an initial cross-polarization from ^{19}F to ^{29}Si prior to beginning the REDOR portion of the sequence, the relaxation was governed by the much shorter ^{19}F T_1, and presaturation was not necessary.

nucleus in these experiments, and the T_1 values for the silicons in octadecasil are relatively long (ca. 20 s), an initial presaturation sequence was incorporated to allow a more efficient recycling time, while still ensuring quantitative reliability. In experiments which utilized an initial cross-polarization from ^{19}F to ^{29}Si prior to beginning the REDOR portion of the sequence, the repeat time was governed by the much shorter ^{19}F T_1 (Table 2), and presaturation was not necessary.

REDOR Experiments on the D4R Silicons (T-1 Si). Experimental REDOR results for the Si in the T-1 site using the two sequences of Figure 4 are shown in Figure 5. The experimental values of $\Delta S/S_0$ did not reach the theoretical maximum of about 1.05 during the first 4.5 ms of dipolar evolution but seemed to oscillate around 0.85–0.92. The explanation for this is that only about 90% of the D4R units contain a fluoride ion, as determined by elemental analysis. This would allow signals from ^{29}Si nuclei in D4R units without fluoride anions to contribute to the intensity of the peaks in the off-resonance (S_0) experiments, which limits the value of $\Delta S/S_0$ attainable. In the case of octadecasil then, these maximum normalized $\Delta S/S_0$ intensities provide a direct method for estimating the percentage occupancy of the D4R units by fluoride ions.

The oscillations observed for the T-1 silicons at short contact times in the CP experiments justify the analysis of the REDOR behavior for these silicons in terms of an isolated ^{29}Si$-^{19}$F spin-pair. To permit fitting of the data, the theoretical values of $\Delta S/S_0$ were multiplied by a scaling factor to account for the incomplete occupancy. This scaling factor does not affect the "period" of the oscillation from which the distance is deter-

mined. Nonlinear least-squares fitting of the REDOR data for the T-1 Si included this scaling factor as a variable and gave an average value for the dipolar coupling of 1150 Hz (standard deviation 50 Hz). This corresponds to a Si$-$F distance of 2.69 $\pm$ 0.04 Å, in excellent agreement with the value of 2.63 Å determined from the X-ray structure. The plots in Figure 5 illustrate how well the scaled theoretical curves (solid lines) calculated using the dipolar couplings and scaling factors determined from the fitting match the observed experimental data. REDOR experiments with an initial cross polarization from ^{19}F to ^{29}Si, followed by a sequence identical to that shown in Figure 4b (but without the presaturation), were also successful (Figure 5a, open circles).

A drift toward a $\Delta S/S_0$ value of unity at longer dephasing times (>4.5 ms, $n > 12$) is seen in Figure 5a (open circles). This probably arises from the dipolar couplings between the T-1 silicons and the next closest (>7 Å) fluoride ions, whose contributions take a much longer time to build up. It is also apparent that data acquired using the pulse sequence with a single dephasing pulse on the unobserved nuclei attain a somewhat higher maximum $\Delta S/S_0$ ratio (ca. 0.92) compared with the value of ca. 0.85 if the train of dephasing pulses was applied to the unobserved nuclei. This small difference in efficiency between the two pulse sequences may be due to resonance offset effects. However the curve fitting for both experiments yielded exactly the same value for the ^{29}Si$-^{19}$F dipolar coupling within experimental error. It should be noted that this may not be the case for other ^{19}F-containing systems, e.g., fluoro-organic sorbates, where there may exist large chemical shift anisotropies, ^{19}F homonuclear, and ^{1}H$-^{19}$F heteronuclear line broadening
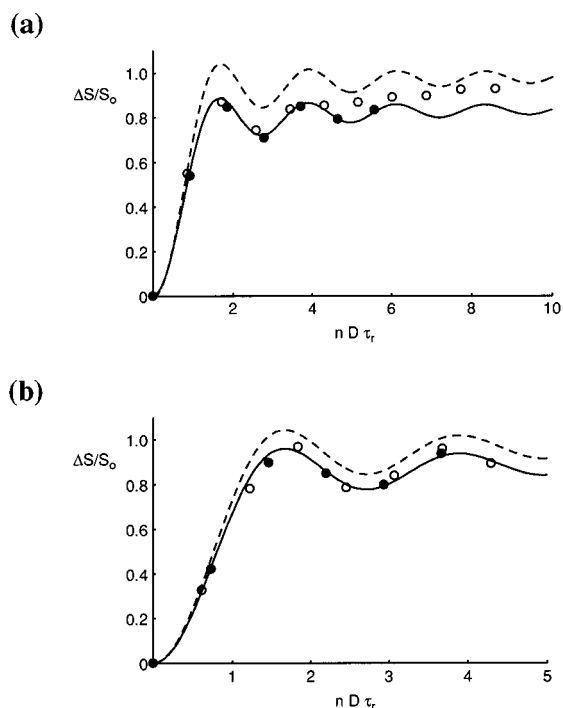
(a)

(b)

Figure 5. REDOR data and fits for the T-1 silicon resonance acquired using different pulse sequences. The theoretical curves were calculated assuming a dipolar coupling of 1150 Hz and either complete (broken line) or incomplete (solid line) occupancy of the D4R by fluoride ions. (a) Dephasing pulses on ^{19}F, spinning speeds of 2.480 kHz (filled circles) and 2.675 kHz (open circles). Solid curve calculated for 85% occupancy. (b) Dephasing pulses on [29]Si, spinning speeds of 3.090 kHz (filled circles), and 3.745 kHz (open circles). Solid curve calculated for 92% occupancy.

interactions. In such cases the choice of pulse sequence may be critical in obtaining the most reliable measurement of D.

REDOR Experiments on Silicons Not in the D4R (T-2 Si). For the T-2 silicons, the [19]F–[29]Si dipolar coupling was estimated to be 122 Hz from the Si–F distance of 5.69 Å calculated from the crystal structure. However, depending on the exact occupancy of the D4R units, there can be up to four fluoride anions in a tetrahedral arrangement about each T-2 silicon and therefore equidistant from it (Figure 1b). This represents a more complicated situation than for the Si in the D4R (T-1 site) as the experiment no longer involves a single, isolated spin-pair. Coupling to several fluorines can produce extra dephasing which translates into a stronger apparent dipolar coupling and thus to an underestimate of the true heteronuclear distance. The theoretical curve calculated for a single, isolated [29]Si–[19]F spin-pair with a dipolar coupling of 120 Hz (not shown) does not fit the experimental data at all, but a reasonable fit assuming an *I-S* spin pair could be obtained with $D = 220$ Hz, corresponding to a Si–F distance of 4.67 Å. This is much shorter than that known from the X-ray structure, and it illustrates a potential problem when multiple spins are involved and no clear oscillation is observed.

When an observed spin magnetization is dephased by dipolar interactions with more than one other spin, the dephasing will normally be dominated by the nearest one (since $D \propto 1/r^3$). However, when the distances are comparable, dephasing from multiple spins will be cumulative.[54,57] Several approaches which permit the calculation of the REDOR behavior for systems where multiple spins are dipolar coupled to the observed nucleus have been reported.[54,56,57,59,62] Naito et al.[57] detailed the derivation of an expression for a three spin system based on the summation of two pairwise interactions with permutations

of the possible spin states. They demonstrated that the geometrical arrangement of the spin-pairs had a measurable effect on the calculated curves. Schaefer and co-workers[56,59] derived a more general equation for the REDOR behavior of an *S* spin dipolar coupled to any number of *I* spins provided that the geometric arrangement of these spins is known. This is also based on the addition of pairwise interactions. Further, Schaefer et al. were able to formulate their final equations for multispin REDOR in terms of a product of cosine terms, rather than as the sum of cosine sums. The product representation gives a substantial improvement in the efficiency of the computations, and this efficiency becomes progressively larger as the number of spin-pairs involved increases. Calculation of theoretical dephasing of a single [29]Si by multiple [19]F's was undertaken for the T-2 silicons assuming an exact tetrahedral arrangement as outlined below. Additional corrections for the partial occupancy of each D4R unit were also incorporated.

Calculation of *S*-Spin Dephasing by Multiple *I*-Spins. For a collection of two or more *I*-spins dipolar coupled to an observed *S*-spin, three angles are required to produce all possible relative orientations of the internuclear vectors in a spinning powder sample. While it is possible to parameterize a multiple spin system by specifying the spherical polar angles (α, β), of the axis of rotation and a third angle γ to define the angle of the rotation about this axis (Figure 3b), it is more convenient to use the Euler angles (ϕ, θ, ψ) as this simplifies the calculations required to perform the vector rotations.

The calculation of multinuclear dephasing is based on the additivity of exponential products[73] and requires a knowledge of the relative geometry as well as the internuclear distances.[57,59] Where structural information is known this can be incorporated, otherwise a model of the spin cluster must be proposed. The dephasing of a single observed [29]Si spin dipolar coupled to more than one ^{19}F spin can be calculated directly[56] as the powder average of a sum of independent dephasings assuming that the fluorines are not coupled to each other and that the fluorine dephasings of the silicons are independent of one another. For octadecasil the first condition is satisfied because the sample is undergoing magic angle spinning at speeds (2–5 kHz) that greatly exceeded the largest homonuclear [19]F–[19]F dipolar coupling (130 Hz for 9.3 Å separation). The second condition is assumed to hold because of the good fits obtained in other systems[56,57,59] and for the T-1 silicons in the present work.

For a REDOR experiment on an isolated *I-S* spin pair with two dephasing π-pulses per rotor cycle positioned at one-half and complete rotations of the spinner, $\Delta\Phi$ is given by eq 3. When two or more spin-$^1/_2$ nuclei dipolar coupled to the observed spin-$^1/_2$ nucleus it is necessary to express $\Delta\Phi$ in terms of the three Euler angles. $\mathbf{v} = \{v_1, v_2, v_3\}$ is defined to be a vector of unit magnitude which lies along the heteronuclear vector and $\mathbf{x}$, $\mathbf{y}$, and $\mathbf{z}$ to be unit vectors along the principal axes of the coordinate system ($\mathbf{z}$ is coincident with the spinner axis). A rotation of $\mathbf{v}$ through (ϕ, θ, ψ) gives $\mathbf{v}' = \mathbf{R}(\phi, \theta, \psi)$ $\mathbf{v}$ where $\mathbf{R}(\phi, \theta, \psi)$ is a 3×3 rotation matrix defined as a rotation about the *z*-axis by ϕ, followed by a rotation about the *y*-axis by θ, and then a rotation about the *z*-axis by ψ.[74] The following functions of the spherical polar angles α and β can be defined in terms of the dot products of these vectors:[56]

(72) Garbow, J. R.; Gullion, T. *J. Magn. Reson.* **1991**, *95*, 442.
(73) Boyce, J. B. Ph.D. Thesis, University of Illinois at Urbana-Champaign, U.S.A., 1972.
(74) Arfken, G. *Mathematical Methods for Physicists*; Academic Press: New York, 1985; Chapter 4.

$$\sin\beta \cos\alpha = \mathbf{v'}\cdot\mathbf{x} \qquad (4)$$

$$\sin\beta \sin\alpha = \mathbf{v'}\cdot\mathbf{y} \qquad (5)$$

$$\cos\beta = \mathbf{v'}\cdot\mathbf{z} \qquad (6)$$

Using these identities gives

$$\sin\beta \cos\beta \sin\alpha = (\mathbf{v'}\cdot\mathbf{y})(\mathbf{v'}\cdot\mathbf{z}) \qquad (7)$$

$\Delta\Phi$ can thus be expressed (neglecting any homonuclear interactions) as

$$\Delta\Phi(\phi, \theta, \psi, \lambda) = 32^{1/2}\,\lambda(\mathbf{v'}\cdot\mathbf{y})(\mathbf{v'}\cdot\mathbf{z}) \qquad (8)$$

where

$$(\mathbf{v'}\cdot\mathbf{z}) = v_1(\cos\phi\,\sin\theta) + v_2(\sin\theta\,\sin\phi) + v_3\cos\theta$$

$$(\mathbf{v'}\cdot\mathbf{y}) = v_1(-\cos\psi\,\sin\phi - \cos\theta\,\cos\phi\,\sin\psi) +$$
$$v_2(\cos\phi\,\cos\psi - \cos\theta\,\sin\phi\,\sin\psi) + v_3(\sin\theta\,\sin\psi)$$

For a system of N independent nuclei interacting with a single observed nucleus, there will be N dipolar couplings, D_i ($i = 1$ to N), needed to account for the different heteronuclear distances. We must determine the $\Delta\Phi$'s for all possible combinations of $\sum \pm |D_i|$, recognizing that the individual $\pm^1/_2$ spin states occur with equal probability so there are 2^N combinations of $\sum D_i$ (or $\sum \lambda_i$). Because the sample is a powder, we must average these sums over space (indicated by the angular brackets) to account for the possible crystallite orientations (assumed to be isotropic), add them together, and divide by the number of combinations, c (eq 9). Equation 9 is thus a sum of the appropriate powder averaged sums.

$$\Delta S/S_0 = 1 - c^{-1}\sum_j\langle\cos[\sum_i\Delta\Phi(\phi, \theta, \psi, \lambda_i)]\rangle_{\text{space}}$$
$$(j = 1 \text{ to } c) \quad (9)$$

If we consider the case where two I spins interact with a single observed S spin, we have two dipolar couplings (D_1 and D_2), $N = 2$, and $c = 2$. REDOR experiments yield only the magnitude and not the sign of D, and since $|D_1 + D_2| = |-D_1 - D_2|$, the number of terms in the sums can be reduced by a factor of 2. The averaging over space is accomplished by numerical integration over the three Euler angles, with ϕ and ψ varied from 0 to 2π and θ from 0 to π. Additional factors are needed to normalize the integral ($1/8\pi^2$) and to account for the statistical (spherical) distribution of the spins in a powder about the spinning axis vector ($\sin\theta$). A step size of one degree (or less) is desirable, but larger step sizes may be used to reduce the computation time and still provide acceptable accuracy. For such a three-spin system eq 9 becomes

$$\Delta S/S_0 = 1 - (4\pi^2)^{-1}[\int_\psi\int_\theta\int_\phi\{\cos[\Delta\Phi(\phi, \theta, \psi, +\lambda_1) +$$
$$\Delta\Phi(\phi, \theta, \psi, +\lambda_2)]\}\,d\phi\,\sin\theta\,d\theta\,d\psi +$$
$$\int_\psi\int_\theta\int_\phi\{\cos[\Delta\Phi(\phi, \theta, \psi, +\lambda_1) +$$
$$\Delta\Phi(\phi, \theta, \psi, -\lambda_2)]\}\,d\phi\,\sin\theta\,d\theta\,d\psi] \quad (10)$$

The dephasing can also be calculated as a product over the N dipolar interactions, with spatial (powder) averaging.[56,59] In this form (eq 11) it is no longer necessary to consider the two possible signs of the dipolar couplings as this is implicitly included.[59] This considerably reduces the number of calculations required and thus the computation time. This efficiency gain in the computations gets progressively larger as the number
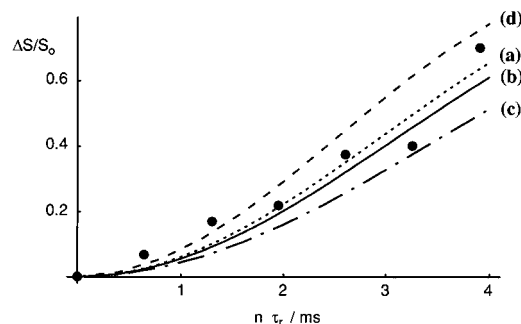

Figure 6. REDOR data for T-2 silicon site acquired at a spinning speed of 3.090 kHz and theoretical curves calculated for dephasing of a single ^{29}Si by multiple ^{19}F nuclei. (a) Exact tetrahedral arrangement of four fluoride anions about each T-2 silicon assuming a Si−F internuclear distance of 5.71 Å ($D = 120$ Hz). (b) A 90% binomial distribution of (up to) four fluoride ions ($r = 5.71$ Å) in a (partial) tetrahedral arrangement about the T-2 silicons. Curves calculated for tetrahedral arrangements of four fluoride anions about each T-2 silicon assuming Si−F internuclear distances of (c) 6.07 Å ($D = 100$ Hz) and (d) 5.43 Å ($D = 140$ Hz) indicate the upper and lower uncertainty limits estimated for the Si−F distance.

of spin-pairs included increases.

$$\Delta S/S_0 = 1 - (8\pi^2)^{-1}\int_\psi\int_\theta\int_\phi(\Pi_i\cos[\Delta\Phi_i(\phi, \theta, \psi, \lambda_i)])$$
$$d\phi\,\sin\theta\,d\theta\,d\psi \quad (i = 1 \text{ to } N) \quad (11)$$

The analysis will be less straightforward for pulse placements other than those described here because, in general, the functions describing the dephasing are more complicated. The validity of programs written to perform the calculations based on eqs 9 and 11 was checked by comparing the results for a variety of three-spin geometries against the data presented in ref 57.

Fitting the REDOR T-2 Data. The theoretical curves calculated for an exact tetrahedral arrangement of four ^{19}F nuclei about a central ^{29}Si using eqs 9 and 11 with $D = 120$ Hz fit the experimental data for the T-2 Si quite well (Figure 6a). In a further refinement the effect of incomplete occupation of the D4R units by fluoride anions was included. This was achieved by assuming contributions from four, three, two, and one equivalent, noninteracting fluorine nuclei, coupled ($D = 120$ Hz) to a single T-2 ^{29}Si nucleus. Curves were calculated for these four sets of ^{29}Si−^{19}F spin-pairs assuming that each T-2 silicon was surrounded by a (partial) tetrahedral arrangement of (up to) four equidistant ^{19}F nuclei. The normalized $\Delta S/S_0$ values thus determined were then multiplied by an appropriate weighting factor and added together produce the final theoretical REDOR curves. The weightings were determined assuming a binomial distribution of fluoride anions in the D4R units with a probability p that a fluoride anion occupies any given D4R. The probability, P_q, that q of the four D4R units surrounding a given T-2 Si are occupied is[75]

$$P_q = C_q(p)^q(1-p)^{4-q} \qquad (12)$$

where C_q is the number of ways of obtaining q occupied D4R units

$$C_q = 4!/q!\,(4-q)! \qquad (13)$$

For $p = 0.9$ eq 12 yields $P_4 = 0.6561$, $P_3 = 0.2916$, $P_2 = 0.0486$, $P_1 = 0.0036$, and $P_0 = 0.0001$. Including the effect of incomplete occupation of the D4R units gives a small improve-

(75) Mendenhall, W.; Beaver, R. J. *Introduction to Probability and Statistics*, 9th ed.; Duxbury Press: California, 1994; p 167.
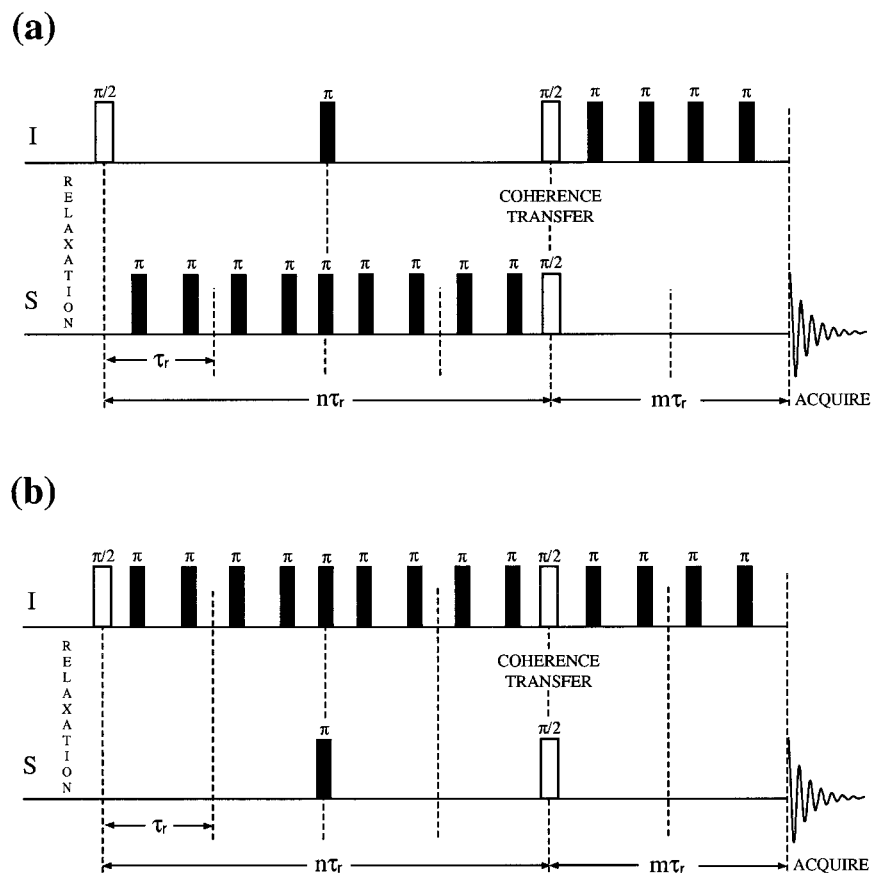
(a)

(b)

Figure 7. The TEDOR pulse sequences used. (a) Dephasing pulses on the observed nuclei before coherence transfer and on the unobserved nuclei after. (b) All dephasing pulses applied to the unobserved nuclei. The number of rotor periods before the coherence transfer (n) could be kept constant and the number of periods after transfer (m) incremented or vice versa. The incrementation of n and m as well as the positions of the dephasing pulses can be adjusted as described in the text.

ment in the goodness of fit (Figure 6b); however, the experimental data are not of good enough quality to permit the occupancy to be determined to an accuracy of better than 5−10%.

It was apparent that the calculated multiple-spin REDOR curves had a much stronger dependence on the magnitude of the dipolar coupling than on the occupancy, and due to the complexity of these calculations, nonlinear least squares fitting was not attempted. The uncertainty in D was estimated to be less than 20 Hz from inspection of curves calculated assuming 100% occupancy of the D4R units and a range of dipolar couplings (Figure 6c,d). Thus, the REDOR fits for the T-2 Si yield a Si−F distance of 5.7 ± 0.4 Å, in very good agreement with the value of 5.69 Å determined from the X-ray crystal structure. This analysis is also in good agreement with the maximum dephasing observed in the REDOR experiments for the T-1 silicons and indicates that the actual occupancy of the D4R units is probably slightly higher than 85%.

These results demonstrate that these complete analyses are reliable and should work for any geometrical arrangement, provided this is known. Although in the case presented here (T-2 Si in octadecasil), all of the *I*-*S* distances were equal, the method outlined above accommodates different distances within the group of nuclei. It should be emphasized that, in general, correct analysis of REDOR results for systems which are simultaneously dipolar coupled to two or more spins is critically dependent on a knowledge of not only the number of nuclei involved but also their specific internuclear distances and geometric relationships. If these are not known, they must be postulated, and consequently the unambiguous nature of the

direct distance determinations for isolated spin-pairs (as is the case for the T-1 silicons) is lost.

TEDOR Experiments. TEDOR experiments were originally developed as an alternative to REDOR to measure the heteronuclear dipolar coupling between nuclei while eliminating unwanted background signals from uncoupled spins,[52,53] which is particularly important for ^{13}C in organic and biological systems. The TEDOR experiment involves two time periods of dipolar dephasing: one before the transfer of coherence (achieved by simultaneous $\pi/2$ pulses) and another after the coherence transfer where the antiphase magnetization is allowed to evolve back into observable magnetization (Figure 7). This allows more permutations, which give the added flexibility of being able to select the experiment best suited to the T_1 and T_2 relaxation values of a particular system. This flexibility may be particularly useful, especially if one T_2 value is unacceptably short, as is often the case for inorganic solids.

In contrast to the REDOR experiment where the loss in intensity arising from dipolar coupling is measured, the TEDOR experiment utilizes coherence transfer to directly observe the magnetization generated, through the dipolar coupling mechanism, and transferred from the unobserved to the observed spins. The TEDOR signal S_T (for an isolated heteronuclear spin-pair) arising from placement of the dephasing π-pulses at one-quarter and three-quarters of a rotor cycle is described by eqs 14−16.[53,55] The integration limits are $\alpha \in [0, 2\pi]$ and $\beta \in [0, \pi]$, n is the number of rotor cycles before the coherence transfer, m is the number of rotor period after the transfer, $\lambda_n = nD\tau_r$, and $\lambda_m = mD\tau_r$.

$$S_T = (4\pi)^{-1} \int \int \sin[\Delta\Phi_n(\alpha, \beta, \lambda_n)] \, \sin[\Delta\Phi_m$$
$$(\alpha, \beta, \lambda_m)] \, \sin\beta \, d\beta \, d\alpha \quad (14)$$

where

$$\Delta\Phi_n(\alpha, \beta, \lambda_n) = 32^{1/2} \, \lambda_n \, \sin\beta \, \cos\beta \, \cos\alpha \quad (15)$$

and

$$\Delta\Phi_m(\alpha, \beta, \lambda_m) = 32^{1/2} \, \lambda_m \, \sin\beta \, \cos\beta \, \cos\alpha \quad (16)$$

Theoretical TEDOR Curve Families and Experimental Considerations. Several families of theoretical TEDOR curves were simulated using the appropriate analytical functions.[55] These included variation of n with m fixed for different values of m, n fixed with m varied, different rotor speeds, dipolar couplings, and several values of the parameter used to "dampen" the curves to account for the homogeneous (T_2) decay that occurs after the coherence transfer.[53] The position of the initial maximum in the curves is shifted to higher number of rotor periods as the spinning rate increases or as the magnitude of the dipolar interaction decreases. Calculation of a series of curves with appropriate parameters corresponding to the experimental conditions prior to beginning TEDOR experiments proved to be a valuable aid for determining the best experimental variables to use. For a given spin system certain values of n or m may be preferable depending on nuclear relaxation parameters and experimental constraints. Variation of m with n fixed can provide more data points in the region of the first maximum of the curves where signal intensities are generally of higher accuracy if refocussing is not used in the second part of the pulse sequence. If possible, it is best to acquire several "periods" of the oscillation to verify the accuracy of the D values.

A simple alternative available for optimizing the experiments for a specific sample is to use different spinning speeds, and another option is to change the positions within each rotor cycle where the dephasing π-pulses are applied. For example they can be at $\tau_r/3$, $2\tau_r/3$ before coherence transfer and $\tau_r/4$, $3\tau_r/4$ after or at $\tau_r/4$, $3\tau_r/4$ before transfer and $\tau_r/5$, $4\tau_r/5$ after. If the pulses are shifted from $\tau_r/4$ and $3\tau_r/4$, appropriate theoretical functions must be determined, and numerical integrations are required to calculate the theoretical TEDOR curves.

It is also important to take into consideration the nuclear relaxation parameters of the nuclei as these limit the range of n or m values that will give viable signal intensities. During the period before coherence transfer, the spin–spin relaxation rate, T_2, of the source nuclei (e.g., ^{19}F) is important, and after the transfer it is the T_2 of the observed nuclei (e.g., ^{29}Si) that limits the maximum time (and thus the number of rotor periods) after coherence transfer that signal can be detected. Because the TEDOR pulse sequences used in the present work all contain an additional π-pulse which generates a spin-echo, it is T_2 rather than T_2^* for the source nuclei that is important.

^{19}F–^{29}Si TEDOR Experiments. Variations of the TEDOR experiment included the application of π-pulses on ^{29}Si, or ^{19}F before the coherence transfer pulse, varying the spinning speed, the position of the pulses, and the number of rotor cycles before and after the transfer pulse. The pulse sequences used for experiments (Figure 7) were such that the minimum increment allowed for the number of rotor cycles before coherence transfer was two because of the use of the simultaneous π-pulses to form an echo to ensure that the chemical shifts are refocussed at the transfer point. Larger increments are possible but only in even numbers of rotor cycles, 4, 6, 8, etc. For the number
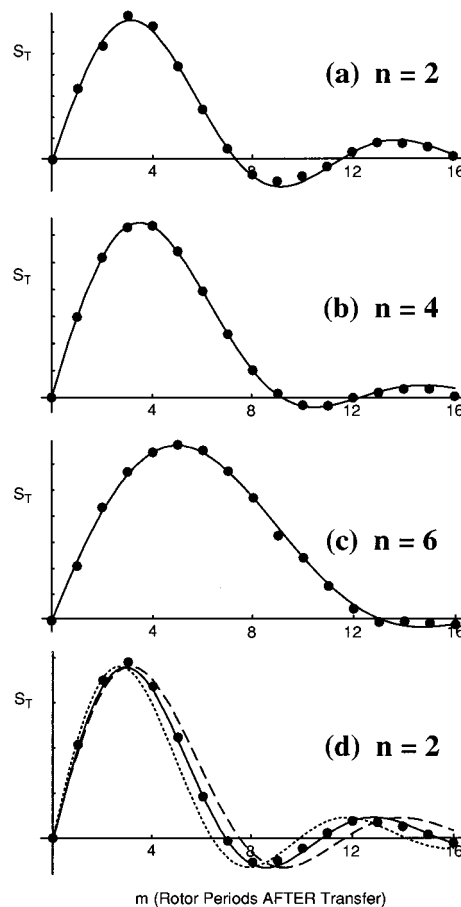

Figure 8. TEDOR data and dipolar couplings (D) determined from nonlinear least-squares fitting of the curve for the T-1 silicon site by varying m with n fixed and all dephasing pulses applied at $\tau_r/4$ and $3\tau_r/4$. (a) $n = 2$, spinning speed 4.770 kHz, $D = 1131$ Hz, (b) $n = 4$, spinning speed 4.770 kHz, $D = 1100$ Hz and (c) $n = 6$, spinning speed 5.244 kHz, $D = 1077$ Hz. (d) Indication of the accuracy of the fit for $n = 2$, spinning speed 4.296 kHz. The curves were calculated assuming dipolar couplings of 1000 Hz (dashed line), 1100 Hz (solid line), and 1200 Hz (dotted line). An exponential dampening of 70 Hz was applied to all curves to account for T_2 decay during the period after the coherence transfer pulses.

of rotor cycles after coherence transfer, increments of 1, 2, 3, or more were permitted since no simultaneous refocussing π-pulses were applied in this part of the sequence. All TEDOR experiments were performed with one of the silicon signals set exactly on resonance.

TEDOR Experiments on the Silicons in the D4R (T-1 Si). TEDOR data obtained for the T-1 silicons with all dephasing pulses at $\tau_r/4$ and $3\tau_r/4$ with the number of rotor cycles after the coherence transfer varied, and the number of rotor cycles before fixed are presented in Figure 8 for several n values. The overlaid theoretical curves were calculated from nonlinear least-squares fitting assuming a single ^{19}F–^{29}Si spin-pair. Because the TEDOR signal intensity S_T is not normalized as it is for REDOR experiments, the experimental intensities were scaled to match the maxima of the theoretical curves. In order to obtain a good match to the experimental intensities at higher numbers of rotor periods, the theoretical curves were also dampened by multiplying them by an exponential factor corresponding to 70 Hz to account for homogeneous spin–spin decay during the period after transfer which is consistent with the observed ^{29}Si line widths (FWHH ≈ 60 Hz). During the analysis of data from different TEDOR experiments, this dampening factor was found to vary slightly, but typically it was in the range 60 ± 20 Hz. Figure 8d shows T-1 Si TEDOR data for $n = 2$ and m varied
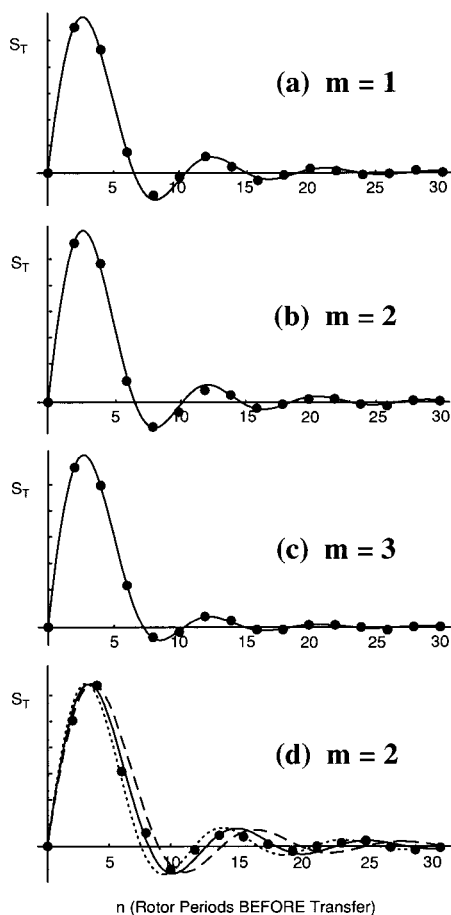
[19]F/[29]Si Distance Determinations in Octadecasil

J. Am. Chem. Soc., Vol. 119, No. 50, 1997   12221

Figure 9. TEDOR data and dipolar couplings (**D**) determined from nonlinear least-squares fitting of the T-1 silicon behavior as a function of n for different (fixed) m values. The spinning rate was 4.540 kHz, and all dephasing pulses at $\tau_r/4$ and $3\tau_r/4$. (a) $m = 1$, **D** =1176 Hz, (b) $m = 2$, **D** = 1207 Hz, and (c) $m = 3$, **D** = 1213 Hz. (d) Indication of the sensitivity of the fit for $m = 2$, spinning speed 5.244 kHz. The curves were calculated assuming dipolar couplings of 1000 Hz (dashed line), 1100 Hz (solid line), and 1200 Hz (dotted line). An exponential dampening of 70 Hz was applied to all curves to account for T_2 decay during the period after the coherence transfer pulses.

Table 3. Comparison of the Dipolar Couplings (**D**) and [19]F−[29]Si Interatomic Distances (**r**) for Octadecasil Determined by Various Methods[e]

		method		
T-site	parameter	TEDOR[a]	REDOR[a]	X-ray[b]
T-1	**D**/Hz	1130 (50)	1150 (50)	1234 (5)
(Si in D4R)	r/Å	2.70 (0.04)	2.69 (0.04)	2.630 (0.003)
T-2	**D**/Hz	120 (20)[d]	120 (20)[d]	122 (5)
(Si not in D4R)	r/Å	5.7 (0.4)[d]	5.7 (0.4)[d]	5.688 (0.003)

[a] Dipolar couplings determined from nonlinear least-squares fitting of experimental data and internuclear distances calculated from these. [b] Distances determined from the single crystal X-ray data of Caullet et al.[28] and dipolar couplings calculated from these. [c] Dipolar couplings determined from visual fitting of experimental data and internuclear distances calculated from these. [d] Standard deviation estimated from visual fittings. [e] Standard deviations are given in parentheses.
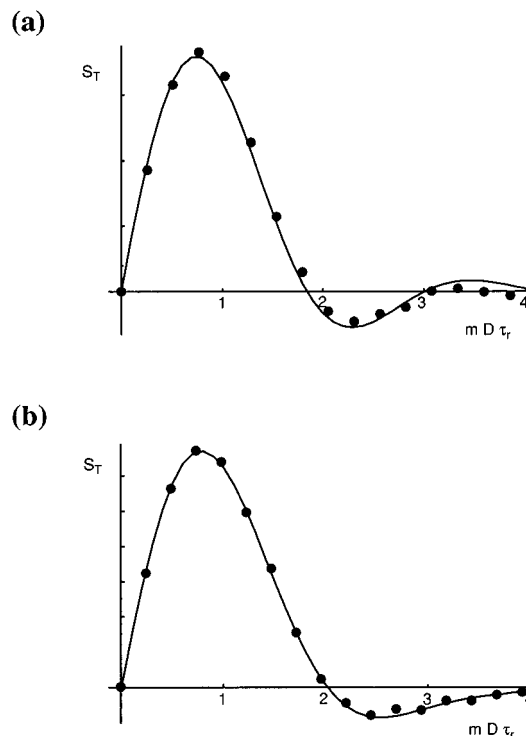
(a)

(b)

Figure 10. TEDOR data and fits for the T-1 Si with all of the dephasing pulses before coherence transfer at $\tau_r/4$ and $3\tau_r/4$ and those after the transfer positioned at (a) $\tau_r/5$, $4\tau_r/5$ and (b) $\tau_r/6$, $5\tau_r/6$. The number of rotor periods before transfer was fixed at 2, m was varied as indicated, and the spinning speed was 4.285 kHz. The theoretical curves were calculated for a dipolar coupling of 1100 Hz with an exponential dampening of 70 Hz to account for T_2 decay.

together with theoretical curves calculated assuming dipolar couplings of 1000 Hz (dashed line), 1100 Hz (solid line), and 1200 Hz (dotted line). Clearly the quality of the fits is excellent, with less than 100 Hz uncertainty in **D**.

Figure 9 shows the data obtained for the T-1 Si when n was varied and m was fixed. The experimental data again agree closely with the theoretical curves determined from nonlinear fitting. Furthermore, because in these experiments there are more "periods" of the oscillation to fit, these represent a quite stringent test of the fit of the experimental data to the theoretically predicted behavior. To our knowledge this is the first time TEDOR experiments have been reported where n was varied and m fixed. There was no discernible difference between TEDOR experiments performed with the dephasing pulses before the coherence transfer on either [29]Si or [19]F.

Weighted, nonlinear fittings of the TEDOR experiments with all dephasing π-pulses at $\tau_r/4$ and $3\tau_r/4$ yielded an average value of **D** = 1130 Hz with a standard deviation of 50 Hz for the silicons in the D4R units. From these values the Si−F interatomic distance was calculated to be 2.70 ± 0.04 Å, which is slightly longer than the value of 2.63 Å reported from diffraction measurements[28] but still in very good agreement. As seen from Table 3, the Si−F distance for the T-1 silicons determined from TEDOR experiments is in very close accord

to that found from REDOR experiments, and both techniques have comparable accuracy.

Moving the Dephasing Pulses. The TEDOR data obtained by changing the positions of the dephasing pulses from $\tau_r/4$, $3\tau_r/4$ required integration of the appropriate functions describing the dipolar interactions and subsequent numerical point-by point integration of those functions. Results from these experiments were plotted versus the dimensionless parameter $\lambda_n = nD\tau_r$ (or $\lambda_m = mD\tau_r$) so that "universal" curves (for isolated I-S spin pairs) were obtained that could be used for fitting data acquired at different spinning speeds. The resulting curves (calculated using **D** = 1100 Hz and 70 Hz dampening) showed very good agreement with the experimental data. Figure 10 shows data for the T-1 Si and the theoretical curves for TEDOR experiments performed with the dephasing pulses moved to (a) $\tau_r/5$, $4\tau_r/5$ and (b) $\tau_r/6$, $5\tau_r/6$ after the coherence transfer. The dephasing pulses were at $\tau_r/4$ and $3\tau_r/4$ before the transfer. The dipolar

coupling determined from experiments performed with the pulses moved from $\tau_r/4$ and $3\tau_r/4$ was generally less (by about 50 Hz) than that determined for other TEDOR experiments and probably indicates that moving the pulses yields a less efficient TEDOR experiment.

TEDOR Experiments on the Silicons not in the D4R (T-2 Si). TEDOR data for the T-2 Si (not shown) was also well fit by theoretical curves calculated for a tetrahedral arrangement of four fluorides about a central T-2 silicon ($D = 120$ Hz) using multiple spin analysis analogous to that outlined above. This corresponds to $r = 5.71$ Å in good agreement with that determined from the crystal structure and the REDOR experiments. If an isolated $^{29}Si-^{19}F$ spin-pair was assumed, nonlinear least squares fitting to the TEDOR data for the T-2 Si yielded a value of $D = 205$ Hz, which corresponds to a Si–F distance of 4.78 Å, much less than that known from the crystal structure. This result again illustrates the danger of obtaining incorrect internuclear distances from fitting TEDOR experimental data if more than two spins are present and the fitting assumes only a single, isolated spin-pair.

Conclusions

High resolution solid-state NMR experiments can yield considerable information on zeolite framework structures and the geometry of host–guest complexes with fluorine-containing species. The results indicate that accurate, reliable, interatomic Si–F distances for isolated spin-pairs can be determined from the magnitude of the $^{19}F-^{29}Si$ dipolar coupling constants determined from REDOR and TEDOR experiments as summarized in Table 3.

REDOR experiments yield normalized intensities which are useful for testing the goodness of the fit of experimental data to the theory and even in the present case for estimating the percentage occupancy of the D4R units by fluoride ions. TEDOR experiments eliminate unwanted background signals arising from observed nuclei which are not dipolar coupled to the heteronuclear spins and can provide additional advantages because of the larger number of experimental variables available and the corresponding increased flexibility to accommodate large T_1 or small T_2 values of either nucleus. An advantage of TEDOR experiments over REDOR is that it is possible to extend them to 2-D correlation experiments.[64,65,67,76] This could be very useful in cases where there are several resonances for both nuclei as it should permit a differentiation between the connectivities. This will be important for three-dimensional host–guest structure determinations in frameworks of the type studied here.

It is possible to obtain incorrect internuclear distances from fitting REDOR and TEDOR experimental data if more than one spin is dipolar coupled to the observed spin and the fitting assumes only a single, static, isolated spin-pair. Independent information which verifies that the experimental data relates to an isolated spin-pair (e.g., the observation of oscillations at short contact times in a cross-polarization experiment) should be obtained. For spin systems which cannot be considered as isolated spin-pairs (e.g., the T-2 Si in octadecasil), it may be possible to determine the dipolar couplings (and thus distances) accurately from REDOR and TEDOR experiments. However, because there is a strong dependence on the number of spins involved as well as the specific geometrical arrangement and

motions of these direct determination of the dipolar couplings cannot be achieved as it can for isolated spin-pairs, and the experimental data must be fit to a model structure.

Simulations with various clusters of spins have shown that the dephasing is typically dominated by the closest heteronuclear contacts when homonuclear interactions are ignored. If an accurate model which specifies the positions (and motions) of all the spins within a cluster can be proposed, then distances from observed spins to multiple heteronuclear dephasing spins may be inferred. Such a model must explicitly include the number of spins, any motional averaging, the statistical probability that each site is occupied by an NMR-active isotope, the relative spatial arrangement, and the heteronuclear distances. The quality of the model will be determined by the consistency of the theoretical curve to account for the experimentally observed behavior as a function of dephasing time. Because the dephasing predicted for different geometries can be very similar at short dephasing times, it is generally important that data be acquired at sufficiently long dephasing times to permit discrimination between different models. However, other problems associated with the use of long dephasing times such as poor signal-to-noise, relative motions of the spins, and significant dephasing from more distant spins may complicate these analyses. In framework/sorbate host–guest systems, sorbate motions such as diffusion and reorientation will often occur at ambient temperatures on the many milliseconds time scale of the REDOR and TEDOR experiments. However, only in unique situations can such slow motions be detected by NMR,[77] and caution should be exercised when implementing them in this area.

Reliable distance determinations for multiple spin systems may only be obtained with knowledge of the spin cluster geometry, as demonstrated in the present work. If unambiguous distance determinations are needed, the system under investigation should be prepared in a manner that will produce isolated spin-pairs (e.g., by isotopic dilution) if at all possible. The quantitative distance information determined from $^{19}F-^{29}Si$ TEDOR and REDOR NMR enables the precise location of ^{19}F-containing species within framework structures. Such experiments could be extended to determine $^{19}F-^{31}P$ interatomic distances in aluminophosphate molecular sieves (AlPO$_4$'s) with fluorine-containing guests and to other framework/sorbate host–guest complexes. A number of such systems are currently under investigation.

---

(76) Vega, A. J. *J. Am. Chem. Soc.* **1988**, *110*, 1049.

(77) Fyfe, C. A.; Diaz, A. C.; Grondey, H.; Fahey, B. Manuscript in preparation.